

Testing the Maxwell-Boltzmann distribution using Brownian particles

Jianyong Mo, Akarsh Simha, Simon Kheifets and Mark G. Raizen*

Center for Nonlinear Dynamics and Department of Physics
The University of Texas at Austin, Austin, TX 78712, USA

*raizen@physics.utexas.edu

Abstract: We report on shot-noise limited measurements of the instantaneous velocity distribution of a Brownian particle. Our system consists of a single micron-sized glass sphere held in an optical tweezer in a liquid in equilibrium at room temperature. We provide a direct verification of a modified Maxwell-Boltzmann velocity distribution and modified energy equipartition theorem that account for the kinetic energy of the liquid displaced by the particle. Our measurements confirm the distribution over a dynamic range of more than six orders of magnitude in count-rate and five standard deviations in velocity.

© 2015 Optical Society of America

OCIS codes: (120.1880) Detection; (140.7010) Laser trapping; (280.7250) Velocimetry

References and links

1. K. Huang, *Statistical mechanics* (Wiley 1987).
2. Lord Kelvin, "On a decisive test-case disproving the Maxwell-Boltzmann doctrine regarding distribution of kinetic energy," *Proc. R. Soc. London* **51**, 397-399 (1892).
3. R. J. Gould and R. K. Thakur, "Deviation from a Maxwellian velocity distribution in low-density plasmas," *Phys. Fluids*, **14**, 1701-1706 (1971).
4. R. J. Gould and M. Levy, "Deviation from a Maxwellian velocity distribution in regions of interstellar molecular hydrogen," *Astrophys. J.* **206**, 435-439 (1976).
5. D. D. Clayton, "Maxwellian relative energies and solar neutrinos," *Nature* **249**, 131 (1974).
6. T. Li, S. Kheifets, D. Medellin, M. G. Raizen, "Measurement of the instantaneous velocity of a Brownian particle," *Science* **328**, 1673-1675 (2010).
7. S. Kheifets, A. Simha, K. Melin, T. Li, M. G. Raizen, "Observation of Brownian motion in liquids at short times: instantaneous velocity and memory loss," *Science* **343**, 1493-1496 (2014).
8. R. Zwanzig and M. Bixon, "Compressibility effects in the hydrodynamic theory of Brownian motion," *J. Fluid Mech.* **69**, 21-25 (1975).
9. A. B. Basset, "On the motion of a sphere in a viscous liquid," *Phys. Eng. Sci.* **179**, 43-63 (1888).
10. H. J. H. Clercx and P. P. J. M. Schram, "Brownian particles in shear flow and harmonic potentials: A study of long-time tails," *Phys. Rev. A* **46**, 1942-1950 (1992).
11. B. Lukić, S. Jeney, Ž. Sviben, A. J. Kulik, E. L. Florin and L. Forró, "Motion of a colloidal particle in an optical trap," *Phys. Rev. E* **76**, 011112 (2007).
12. A. Ashkin, "Applications of laser radiation pressure," *Science* **210**, 1081-1088 (1980).
13. I. Chavez, R. Huang, K. Henderson, E.-L. Florin, and M. G. Raizen, "Development of a fast position-sensitive laser beam detector," *Rev. Sci. Instrum.* **79**, 105104 (2008).
14. D. Cheng, K. Halvorsen and W. P. Wong, "Note: High-precision microsphere sorting using velocity sedimentation," *Rev. Sci. Instrum.* **81**, 026106 (2010).
15. M. Grimm, S. Jeney, T. Franosch, "Brownian motion in a Maxwell fluid," *Soft Matter* **7**, 2076-2084 (2011).

1. Introduction

The one dimensional Maxwell-Boltzmann distribution (MBD) for the velocities of molecules in an ideal gas in thermal equilibrium is $f(v) = \sqrt{\frac{m}{2\pi k_B T}} \exp\left(-\frac{mv^2}{2k_B T}\right)$, where m is mass, k_B

is Boltzmann's constant and v is the velocity [1]. The energy equipartition theorem $\frac{1}{2}m\langle v^2 \rangle = \frac{1}{2}k_B T$ can be derived from the MBD. The actual velocity distribution in certain systems has been predicted to deviate from the standard MBD, for example, due to particle-particle interactions or relativistic effects [2–5]. A simple thought experiment showing a change in the velocity distribution by adding an arbitrary potential was proposed by Lord Kelvin in 1892 [2]. Deviations from the MBD have been predicted for low density plasmas [3], interstellar molecular hydrogen [4], and in the solar plasma by measuring neutrino flux [5]. In spite of predicted deviations, the MBD still holds as a remarkably robust approximation for most physical systems.

Previous work has reported an experimental verification of the MBD and energy equipartition theorem for a microsphere in air [6]. This result is to be expected, since the interaction of a particle with the surrounding air is fairly weak. In the case of a particle in a liquid, it is not so clear whether the MBD and energy equipartition theorem still hold, due to the strong hydrodynamic coupling. A measurement of the instantaneous velocity of a microsphere in a liquid has been reported [7], however, the sample size (2 million velocity data points) was not sufficient to give a robust estimate of the distribution for velocities beyond 3 standard deviations from the mean.

In this Letter, we report a more accurate test of the MBD and energy equipartition theorem for three systems: a silica (SiO_2) glass microsphere in water, a silica glass microsphere in acetone and a barium titanate glass (BaTiO_3) microsphere in acetone. We find that the velocity distribution follows a modified Maxwell-Boltzmann distribution $f(v) = \sqrt{\frac{m^*}{2\pi k_B T}} \exp\left(-\frac{m^* v^2}{2k_B T}\right)$, where m^* is the effective mass of the microsphere in liquid which is the sum of the mass of the microsphere m_p and half of the mass of the displaced liquid m_f , $m^* = m_p + \frac{1}{2}m_f$ [8]. The liquid adds a virtual mass $\frac{1}{2}m_f$ to the microsphere, since accelerating the microsphere requires a force both on the microsphere and the surrounding liquid. As a result, the energy equipartition theorem also needs to be modified to $\frac{1}{2}m^*\langle v^2 \rangle = \frac{1}{2}k_B T$.

The apparent conflict between our observation and the equipartition theorem can be resolved by considering the effects of compressibility of the liquid [8]. Below timescales on the order of $\tau_c = r/c$, where c is the speed of sound in the liquid and r is the radius of the microsphere, the compressibility of the liquid cannot be neglected and the velocity variance will approach the energy equipartition theorem. The effects of compressibility in our three systems are well separated from the regime of hydrodynamic Brownian motion.

2. Hydrodynamic Brownian motion in a harmonic trap

The translational motion of a spherical particle in a liquid trapped by an optical tweezer can be described by the Langevin equation [10, 11],

$$m^* \ddot{x}(t) = -Kx(t) - 6\pi\eta r \dot{x}(t) - 6r^2 \sqrt{\pi\rho_f \eta} \int_0^t (t-t')^{-1/2} \ddot{x}(t') dt' + F_{th}(t) \quad (1)$$

where K is the trapping strength, η is the liquid viscosity and ρ_f is the liquid density. The first term on the right-hand side of Eq. (1) is the harmonic trapping force, the second term is the ordinary Stokes friction, the third term is the Basset force [9], and the last term is the thermal stochastic force [7]. The mean-square displacement (MSD) of a trapped microsphere, $\langle (x(t+\tau) - x(\tau))^2 \rangle$, is expressed in Eq. (4) in reference [11]. The corresponding position power spectral density (PPSD), $S_x(f)$, which describes the frequency distribution of the Brownian motion of the microsphere, is given in Eq. (12) in reference [11]. The velocity power spectral density (VPSD) can be obtained from PPSD using the relation $S_v(f) = (2\pi f)^2 S_x(f)$. The theoretical cumulative velocity power spectral density (cumulative VPSD) does not have an analytic form but can be obtained by numerically integrating the VPSD up to a given frequency.

3. Experimental setup

A simplified schematic of our experimental setup for measuring the instantaneous velocity of a Brownian particle in a liquid is shown in Fig. 1, containing two main parts: optical trapping [12] and high-bandwidth balanced detection [13]. The details of the setup can be found in

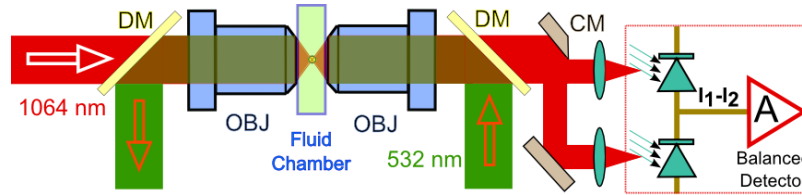


Fig. 1. A simplified schematic of experimental setup for measuring instantaneous velocity of a microsphere trapped by counter-propagating 1064 nm and 532 nm laser beams focused by microscope objectives (OBJ) in liquid. The 1064 nm laser is used to detect the horizontal motion of the particle using a high-power, high bandwidth balanced detector. DM: dichroic mirror, CM: D-shaped mirror.

[7]. A BaTiO₃ microsphere was trapped using counter-propagating dual beams (a 1064 nm laser (Mephisto, Innolight) and a 532 nm laser (Verdi, Coherent)) focused by two identical water-immersion microscope objectives (OM-25, LOMO). Only the 1064 nm laser was used for systems with silica microspheres. In this experiment, the powers of the 1064 nm beam and 532 nm beams were about 300 mW and 200 mW respectively. The 1064 nm laser also served as the detection beam, which was split into two roughly equal halves using a D-shaped mirror. A home-made low noise, high bandwidth, high-power balanced detector was used to amplify the power difference between the halves, which depends on the position of the trapped particle. The total power incident on the detector was about 140 mW for each system.

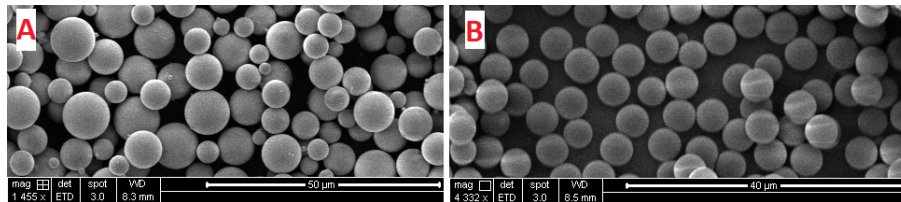


Fig. 2. Scanning electron microscope images of the microspheres (sputtered with about 10 nm Au/Pd with 60/40 ratio) demonstrate high sphericity. A: The widely-dispersed (0.1-10 μm) BaTiO₃ glass microspheres; B: The mono-disperse silica glass microspheres.

Experiments were performed using silica microspheres ($n = 1.46$, $\rho = 2.0 \text{ g/cm}^3$, Bangs Laboratories) and BaTiO₃ microspheres ($n = 1.9$, $\rho = 4.2 \text{ g/cm}^3$, Mo-Sci L.L.C) in either HPLC-grade water ($n = 1.33$, $\rho_f = 0.998 \text{ g/cm}^3$, $\eta = 9.55 \times 10^{-4} \text{ Pa s}$) or acetone ($n = 1.35$, $\rho_f = 0.789 \text{ g/cm}^3$, $\eta = 3.17 \times 10^{-4} \text{ Pa s}$) at $22 \pm 1 \text{ }^\circ\text{C}$. High sphericity of the microspheres is necessary to eliminate the rotational motion contribution due to asymmetry of the microspheres, and was confirmed by scanning electron microscope images (FEI Quanta 650 SEM) as shown in Fig. 2.

The fluid chamber was constructed within a layer of nescofilm (Bando Chemical Ind. LTD., 80 μm thickness) sandwiched between two number 0 microscope coverslips (Ted Pella, $\sim 100 \mu\text{m}$ thickness). The optical trap confines the particle to the center of the chamber, enabling long measurement sequences and avoiding boundary effects.

The voltage signal from the balanced detector was recorded by a 16-bit digitizer (CS1622, GaGe applied) at a sampling rate of 200 MSa/s. The digitizer has an on-board memory of 2^{27}

samples, which enables about 1 s of continuous recording for one continuous trajectory. To see the possible deviation from the MBD in the high velocity tails requires a large number of data points, which are obtained by taking many 1-s trajectories of the same particle. To achieve sufficient statistics, it is necessary to observe a trapped microsphere for hours without contamination. To remove sub-micrometer contaminants from the BaTiO₃ microspheres, a narrower size distribution of the BaTiO₃ microspheres was selected using velocity sedimentation [14]. Contaminants were further reduced by flushing the chamber thoroughly with HPLC-grade acetone after the microspheres were introduced.

4. Results and discussion

We took many trajectories of the same microsphere in the three systems: a silica microsphere in water (677 trajectories), a silica microsphere in acetone (143 trajectories) and a BaTiO₃ microsphere in acetone (43 trajectories). The number of trajectories was limited by the maximum time for which the particles could be trapped without contamination. The voltage to position conversion factor C , trapping strength K as well as particle diameter d were obtained by a least-squares fit of the measured MSD to theory, as shown in Fig. 3(a) for a typical 1-s trajectory. The measured MSD has a slope of 2 (in a log-log plot) at short times, a signature of the ballistic regime of Brownian motion. At high frequency, the signal is dominated by photon shot noise of the detection beam and has a flat spectrum. As a result, the PPSD flattens at high frequency, as shown in Fig. 3(b). The level of shot noise was obtained by a least-squares fit of the measured PPSD to the sum of the theoretical PPSD and a constant noise level. We can reduce shot noise by increasing the detection beam power, but are ultimately limited by the damage threshold of the balanced detector. The fitting results are listed in Table 1 for the three systems. The uncertainty of each fit parameter is determined from the variance in the results of independent MSD and PPSD fits of all measured trajectories for each system.

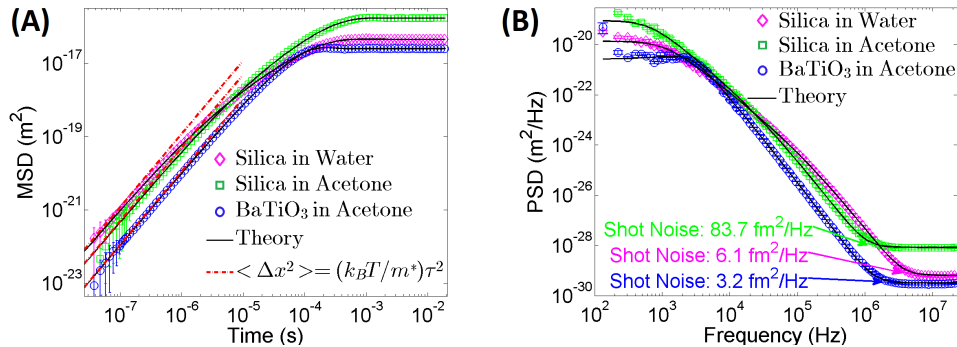


Fig. 3. (A): The MSD of a typical 1-s trajectory for a trapped microsphere in liquid. Red dashed lines indicate the MSD of a particle moving at constant velocity $v_{rms}^* = \sqrt{k_B T / m^*}$; black lines are theoretical MSD. (B): The PPSD for the same trajectories. The PPSD flattens at high frequency due to shot noise of the detection beam at $2.4 fm / \sqrt{Hz}$, $9.1 fm / \sqrt{Hz}$ and $1.8 fm / \sqrt{Hz}$ for a silica microsphere in water, a silica microsphere in acetone and a BaTiO₃ microsphere in acetone respectively. The black line is the sum of theoretical PPSD and a constant shot noise. For both plots: magenta diamonds represent silica in water data; green squares represent silica in acetone data; blue circles represent BaTiO₃ in acetone data.

The VPSD and cumulative VPSD (normalized to $k_B T / m^*$) for the same data as in Fig. 3 are shown in Fig. 4. The cumulative VPSD shows the fraction of velocity signal contained below a given frequency, and can be interpreted as showing the minimum measurement bandwidth necessary to measure the average kinetic energy within a given uncertainty. Magenta lines in

Fig. 4 represent the shot noise contribution as calculated using the results shown in Fig. 3(b). The agreement with the blue data points in each system indicates that it is indeed the dominant source of noise. The cumulative VPSD of the shot noise is proportional to ω^3 , which sets a sharp bandwidth limit, as shown in Fig. 4 (bottom), above which the signal is dominated by noise. The useful bandwidth is not directly limited by the detection bandwidth but by the quantum noise of the detection beam. Instantaneous velocity measurement was made possible by two improvements: first, slowing down the dynamics by using acetone (lower viscosity compared to water) and BaTiO₃ microspheres (higher density compared to silica); and second, improving signal-to-noise by increasing the detected beam power and using BaTiO₃ microspheres (higher refractive index compared to silica improves the scattering efficiency).

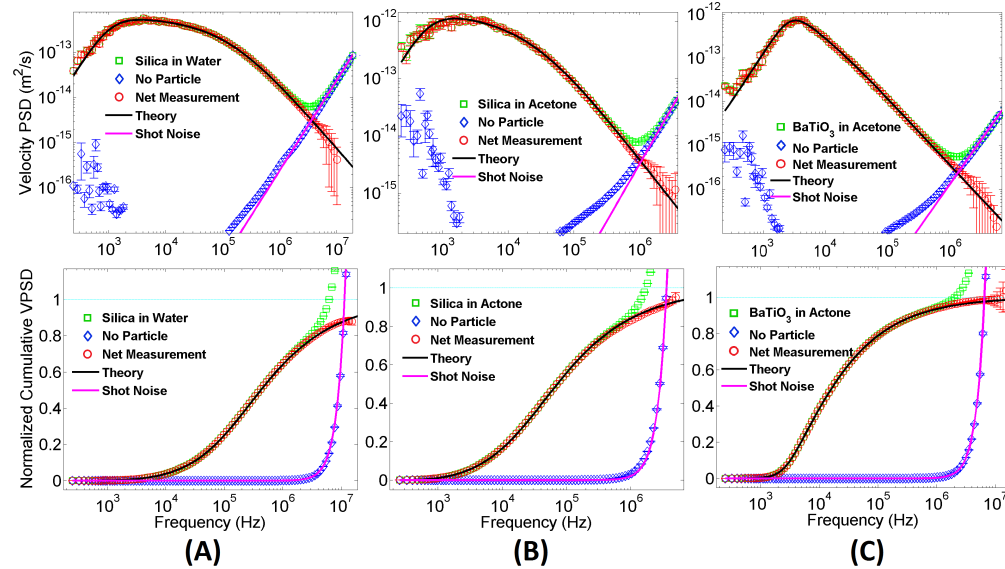


Fig. 4. The VPSD (top) and normalized cumulative VPSD (bottom, normalized to $k_B T / m^*$) of a microsphere in liquid for the same trajectories as in Fig. 3 in three systems, A: a silica microsphere in water; B: a silica microsphere in acetone; C: a BaTiO₃ microsphere in acetone. In all plots: green squares represent the measurements with trapped particles; blue diamonds represent the noise measured without particles present but with the same detection power; red circles represent the net measurement with noise subtracted; black lines are the theoretical prediction; magenta lines are the shot noise using the results shown in Fig. 3(b), indicating that it is the dominant noise source.

The instantaneous velocity of the microspheres was calculated by a numerical derivative of position data, which is averaged using binning. A shorter averaging time would increase the fraction of kinetic energy observed but at the cost of a lower signal-to-noise ratio (SNR), which is defined as $SNR = 10 \log_{10}(\langle v^2 \rangle / \langle n^2 \rangle)$, where $\langle v^2 \rangle$ and $\langle n^2 \rangle$ are the root mean square (rms) values of the velocity and noise measurements. We choose bin size $n = 25, 85$ and 40 for the three systems respectively such that the $SNR \approx 14$ dB for each system. The velocity distributions for three systems, calculated from 3.6 billion, 200 million and 144 million velocity points, are shown in Fig. 5. Blue lines (overlapping almost perfectly with the black line in Fig. 5(c)) are Gaussian fits of the measurements, from which the fraction of mean kinetic energy observed was determined. We observed 78%, 83% and 100% of the mean kinetic energy predicted by the modified energy equipartition theorem, to which the noise contributes about 4%, for the three systems respectively. The three systems give a trend of approaching the instantaneous velocity

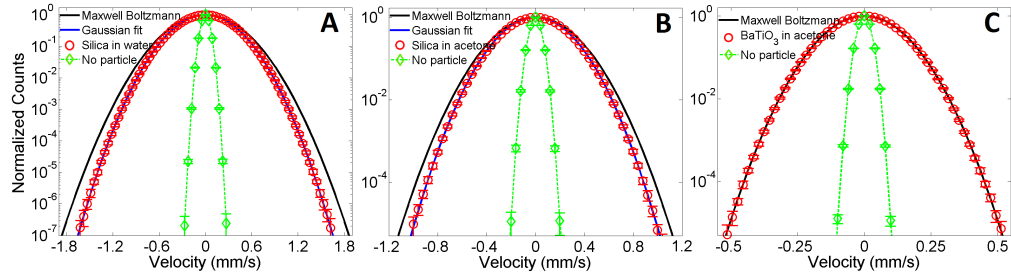


Fig. 5. The normalized velocity distribution for three systems A: a silica microsphere in water ($v_{rms}^* = 327 \mu m/s$); B: a silica microsphere in acetone ($v_{rms}^* = 227 \mu m/s$); C: a BaTiO₃ microsphere in acetone ($v_{rms}^* = 104 \mu m/s$), calculated from 3.6 billion, 200 million and 144 million data points respectively. The histogram bin size for each velocity distribution was set to the rms magnitude of the corresponding noise. For all plots: red circles represent the measurements with trapped microspheres; green diamonds represent the measurements acquired without particles present, but with matching detection power; black lines are the modified MBD predictions; blue lines (overlapping with the black line in C) are Gaussian fits of the measurements, from which the fraction of the mean kinetic energy observed was determined.

measurement, showing the importance of using BaTiO₃ microspheres and acetone.

Table 1. The summary of the results for the three systems.

Systems	Silica in Water	Silica in Acetone	BaTiO ₃ in Acetone
Particle diameter	$3.06 \pm 0.05 \mu m$	$3.98 \pm 0.06 \mu m$	$5.36 \pm 0.06 \mu m$
Trapping strength	$188 \pm 15 \mu N/m$	$50 \pm 8 \mu N/m$	$342 \pm 13 \mu N/m$
Conversion factor (C)	$25.3 \pm 0.5 mV/nm$	$6.3 \pm 0.3 mV/nm$	$31.8 \pm 0.6 mV/nm$
Position shot noise	$2.3 \pm 0.1 fm/\sqrt{Hz}$	$8.9 \pm 0.4 fm/\sqrt{Hz}$	$1.7 \pm 0.1 fm/\sqrt{Hz}$
Velocity data points	3.6 billion	200 million	144 million
Measured kinetic energy	78%	83%	100%

5. Conclusion

In this paper we show that the instantaneous velocity of a microsphere in a liquid follows the modified MBD (and thus, the modified energy equipartition theorem) over a dynamic range of more than six orders of magnitude in count-rate and five standard deviations in velocity. Assuming ergodicity [1], the same conclusion should also be true for an ensemble of identical particles.

To measure the instantaneous velocity in liquid as predicted by the equipartition theorem, the temporal resolution must be shorter than the time scale of acoustic damping, which is around 1 ns for our systems. By using a pulsed laser as the detection beam, one can significantly reduce the shot noise and it may be possible to measure the true instantaneous velocity. Our setup can also be used to measure the velocity distribution of a particle in non-Newtonian fluids [15], where deviations from the modified MBD may result from the viscoelasticity of the solution.

Acknowledgments

The authors acknowledge support from the Sid W. Richardson Foundation and the R. A. Welch Foundation grant number F-1258.